Author(s): Zhang, W.; Cederwall, B.; Doncel, M.; Aktas, Ö.; Ertoprak, A.; Liotta, R.; Qi, C.; Grahn, T.; Nara, Singh B.S.; Cullen, D.M.; Hodge, D.; Giles, M.; Stolze, S.; Badran, H.; Braunroth, T.; Calverley, T.; Cox, D.M.; Fang, Y.D.; Greenlees, P.T.; Hilton, J.; Ideguchi, E.; Julin, R.; Juutinen, S.; Kumar, Raju M.; Li, H.; Liu, H.; Matta, S.; Subramaniam, P.; Modamio, V.; Pakarinen, J.; Papadakis, P.; Partanen, J.;

Title: Lifetime measurements of excited states in 169,171,173Os : Persistence of anomalous B(E2) ratios in transitional rare earth nuclei in the presence of a decoupled i13/2 valence neutron

Year: 2021

Version: Published version

Physics Letters B 820 (2021) 136527

Contents lists available at ScienceDirect

Physics Letters B

www.elsevier.com/locate/physletb

Lifetime measurements of excited states in ^{169,171,173}Os: Persistence of anomalous $B(E2)$ ratios in transitional rare earth nuclei in the presence of a decoupled $i_{13/2}$ valence neutron

W. Zhang [a,*], B. Cederwall [a], M. Doncel [b,c], Ö. Aktas [a], A. Ertoprak [a,d], R. Liotta [a], C. Qi [a], T. Grahn [e], B.S. Nara Singh [f,g], D.M. Cullen [f], D. Hodge [f], M. Giles [f], S. Stolze [e], H. Badran [e], T. Braunroth [h], T. Calverley [e], D.M. Cox [e,i], Y.D. Fang [j], P.T. Greenlees [e], J. Hilton [e], E. Ideguchi [j], R. Julin [e], S. Juutinen [e], M. Kumar Raju [j], H. Li [k], H. Liu [a], S. Matta [a], P. Subramaniam [a], V. Modamio [l], J. Pakarinen [e], P. Papadakis [e,m], J. Partanen [e], C.M. Petrache [n], P. Rahkila [e], P. Ruotsalainen [e], M. Sandzelius [e], J. Sarén [e], C. Scholey [e], J. Sorri [e,o], M.J. Taylor [p], J. Uusitalo [e], J.J. Valiente-Dobón [q]

[a] KTH Royal Institute of Technology, 10691 Stockholm, Sweden
[b] Department of Physics, Oliver Lodge Laboratory, University of Liverpool, Liverpool L69 7ZE, United Kingdom
[c] Department of Physics, Stockholm University, SE-10691 Stockholm, Sweden [1]
[d] Department of Physics, Faculty of Science, Istanbul University, Vezneciler/Fatih, 34134 Istanbul, Turkey
[e] Department of Physics, University of Jyvaskyla, P.O. Box 35, FI-40014 Jyväskylä, Finland
[f] Schuster Building, School of Physics and Astronomy, The University of Manchester, Manchester, M13 9PL, United Kingdom
[g] School of Computing Engineering and Physical Sciences, University of the West of Scotland, Paisley, PA1 2BE, United Kingdom [1]
[h] Institut für Kernphysik, Universität zu Köln, 50937 Köln, Germany
[i] Department of Physics, Lund University, 221 00 Lund, Sweden [1]
[j] Research Center for Nuclear Physics, Osaka University, JP-567-0047 Osaka, Japan
[k] Grand Accélérateur National d'Ions Lourds (GANIL), CEA/DSM–CNRS/IN2P3, F-14076 Caen Cedex 5, France
[l] Department of Physics, University of Oslo, NO-0316 Oslo, Norway
[m] STFC Daresbury Laboratory, Daresbury, Warrington WA4 4AD, United Kingdom [1]
[n] Université Paris-Saclay, CNRS/IN2P3, IJCLab, 91405 Orsay, France
[o] Sodankylä Geophysical Observatory, FI-99600 Sodankylä, Finland [1]
[p] Division of Cancer Sciences, School of Medical Sciences, The University of Manchester, Manchester, M13 9PL, United Kingdom
[q] Istituto Nazionale di Fisica Nucleare, Laboratori Nazionali di Legnaro, I-35020 Legnaro, Italy

ARTICLE INFO

Article history:
Received 13 February 2021
Received in revised form 29 June 2021
Accepted 19 July 2021
Available online 22 July 2021
Editor: D.F. Geesaman

ABSTRACT

Lifetimes of low-lying excited states in the $\nu i_{13/2^+}$ bands of the neutron-deficient osmium isotopes ^{169,171,173}Os have been measured for the first time using the recoil-distance Doppler shift and recoil-isomer tagging techniques. An unusually low value is observed for the ratio $B(E2; 21/2^+ \rightarrow 17/2^+)/B(E2; 17/2^+ \rightarrow 13/2^+)$ in ^{169}Os, similar to the "anomalously" low values of the ratio $B(E2; 4_1^+ \rightarrow 2_1^+)/B(E2; 2_1^+ \rightarrow 0_{gs}^+)$ previously observed in several transitional rare-earth nuclides with even numbers of neutrons and protons, including the neighbouring ^{168,170}Os. Furthermore, the evolution of $B(E2; 21/2^+ \rightarrow 17/2^+)/B(E2; 17/2^+ \rightarrow 13/2^+)$ with increasing neutron number in the odd-mass isotopic chain ^{169,171,173}Os is observed to follow the same trend as observed previously in the even-even Os isotopes. These findings indicate that the possible quantum phase transition from a seniority conserving structure to a collective regime as a function of neutron number suggested for the even-even systems is maintained in these odd-mass osmium nuclei, with the odd valence neutron merely acting as a "spectator". As for the even-even nuclei, the phenomenon is highly unexpected for nuclei that are not situated near closed shells.

* Corresponding author.
E-mail address: wezh@kth.se (W. Zhang).
[1] Present address.

https://doi.org/10.1016/j.physletb.2021.136527

1. Introduction

The emergence of collective behaviour and deformation in atomic nuclei due to the residual interactions between valence particles outside closed-shell configurations represents one of the most important challenges for the description of finite many-body quantum systems [1,2]. Such effects imply that the wave function has spread out over multiple, coherent particle-hole components and are commonly associated with experimental observables such as a lowering of the first excited 2_1^+ state energy accompanied by an increase in the $2_1^+ \rightarrow 0_{gs}^+$ reduced electric quadrupole transition probability, $B(E2)$, in atomic nuclei with even numbers of neutrons and protons. The $E2$ strength between quantum states in the nucleus is a particularly sensitive probe of the corresponding wave functions and it is consequently crucial for understanding collective phenomena. In general, a roughly inverse parabolic evolution of electric quadrupole strength is expected along isotopic chains as the nucleon numbers are varied between closed shells (see, e.g., Ref. [3]). For a closed-shell configuration, the $B(E2)$ value is at a minimum and governed by the individual single-particle degrees of freedom. As the nucleon number deviates from a "magic" number, quadrupole surface vibrations around spherical symmetry first develop. These are generally followed by the gradual evolution of increasingly deformed shapes towards the well-developed axially-symmetric shapes and their associated rotational excitations and maximal $B(E2)$ values when the Fermi level is situated at mid-shell.

The $B(E2)$ values usually increase with spin for the low-lying yrast states within a collective (rotational or vibrational) band structure [2]. As a consequence, the $B(E2; J+4 \rightarrow J+2)/B(E2; J+2 \rightarrow J)$ ratio (hereafter designated as $B_{4/2}$), J being the angular momentum of the lowest state in the band, is strictly larger than unity for collective excitations. For an ideal quantum rotor, a value of $B_{4/2} = 10/7 = 1.43$ known as the Alaga rule is obtained, whereas for a harmonic vibrator, $B_{4/2} = 2$, reflecting the ratio between the number of phonons in the initial state for each transition. The ratio $B_{4/2} > 1$ is also true for descriptions of collective behaviour within algebraic models such as the Interacting Boson Model (IBM) [4]. In principle, the only conceivable exceptions to this rule are structures exhibiting seniority symmetry near "magic" nucleon numbers or shape coexistence. While seniority conservation has previously been considered to be the most likely, albeit unexpected, scenario [5], shape coexistence requires special attention since neutron deficient isotopes of the transition metals are well-known examples of nuclei exhibiting low-lying coexisting structures built on different quadrupole shapes [6,7].

We here report on the first measurement of lifetimes of excited states in ^{169,171,173}Os. Partial level schemes of these nuclei are shown in Fig. 1. The deduced $B(E2)$ values are in qualitative agreement with the trends previously observed for members of the even-N tungsten, osmium and platinum isotopes [5,13–17] with similar neutron numbers.

2. Experimental details

Excited states in ^{169}Os, ^{171}Os, and ^{173}Os were populated in the ^{92}Mo(^{83}Kr, $2pxn$) fusion-evaporation reaction at the Accelerator Laboratory of the University of Jyväskylä (JYFL), Finland. The ^{83}Kr beam was produced and accelerated to 383 MeV by the K130 cyclotron, then bombarded a 0.52 mg/cm^2 thick, isotopically enriched ^{92}Mo target foil, which was stretched and mounted in

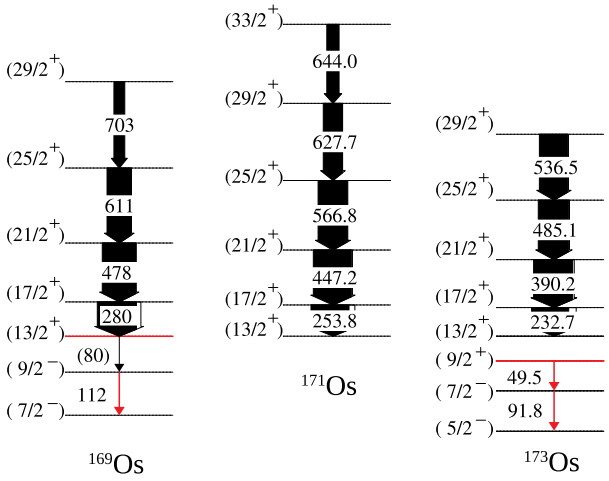

Fig. 1. Partial level schemes built on the $i_{13/2}$ state of ^{169,171,173}Os and the decay paths to the ground states for ^{169,173}Os. The figure has been reproduced from the data of Refs. [8–12]. The widths of the arrows above the $13/2^+$ state are proportional to the relative intensities of the transitions. The states in red depict the isomeric states and the transitions in red were used here for tagging, see details in the text.

the differential plunger for unbound nuclear states (DPUNS) device [18]. The fusion-evaporation residues were slowed down in the 1 mg/cm^2 thick Mg degrader foil of DPUNS to approximately 80% of the initial recoil velocity before they entered the gas-filled electromagnetic ion separator RITU [19]. RITU was used to separate the velocity-degraded recoiling fusion products from unreacted beam particles and unwanted reaction residues and to transport them to the GREAT spectrometer [20] located at its focal plane.

Prompt γ rays at the target position were detected by the JUROGAM II germanium detector array consisting of 15 Eurogam Phase I-type [21] and 24 Euroball clover [22] escape-suppressed detectors, with a total photopeak efficiency of ∼6% at 1.3 MeV. The clover detectors were arranged symmetrically relative to the direction perpendicular to the beam (twelve at 75.5° and twelve at 104.5°), while the Phase I detectors were placed at backward angles with respect to the beam direction (five at 157.6° and ten at 133.6°). The lateral position and kinetic energy loss of the recoils were measured when passing through the multi-wire proportional counter (MWPC) and they were subsequently implanted into two double-sided silicon strip detectors (DSSDs) of the GREAT spectrometer. Meanwhile, the time-of-flight (TOF) between the MWPC and the DSSDs was measured, which was combined with the energy loss in the MWPC to select the recoils from the scattered beam. Located downstream of the DSSDs within the vacuum chamber was a double-sided planar germanium detector [23], which was used to measure predominantly low-energy γ and X rays. The planar detector has an absolute efficiency of up to 30% at 100 keV [20], making it very suitable for the measurement of low-energy delayed or isomeric γ rays.

Using the recoil distance Doppler shift (RDDS) technique [24], lifetimes of excited states were measured at nine different target-to-degrader distances ranging from 11 μm to 2 mm. The data streaming from the JUROGAM II and the GREAT spectrometer were collected and merged using the triggerless Total Data Readout (TDR) data acquisition system with a global 100 MHz clock [25]. Offline sorting and analysis of the measured data were performed using the GRAIN [26] and RADWARE [27] software packages.

3. Results

3.1. ^{169}Os

The first observation of excited states in ^{169}Os was reported by Joss et al. and a collective band was attributed to a single-neutron $i_{13/2}$ configuration [8]. Thornthwaite [9] later proposed the bandhead $13/2^+$ state to be an isomeric state with a half-life of 17.3(12) μs and tentatively assigned a cascade of 80 keV and 112 keV γ-ray transitions to connect the $\nu i_{13/2}$ band to the $7/2^-$ ground state. The rotational sequence in the yrast band and its decay path to the $7/2^-$ ground state is displayed in Fig. 1. In the present experiment, the 112 keV γ-ray transition was clearly observed by the planar detector at the focal plane, while the 80 keV transition was extremely weak and its correlation with 112 keV was barely visible above the background, presumably due to its large internal conversion coefficient. The strong presence of Os K X-rays in coincidence with the 112 keV line in the focal plane germanium detectors supports this assumption. In this work, recoil-isomer tagging (RIT) [28] was employed in order to select the γ-ray transitions of interest from the vast background of γ-rays from more prolific reaction channels. Isomer-delayed 112 keV transitions detected at the focal plane within 30 μs after the recoil implantation were used to select the temporally correlated prompt γ rays of ^{169}Os emitted at the target position. The alternative approach of using recoil-decay tagging (RDT) [29] technique proved in this case to yield insufficient statistics and selectivity due to the low α-decay branching ratio of 11(1)% and the relatively long half-life of 3.6(2) s [30].

In the present study, the lifetimes of the $I^\pi = 17/2^+$ and $21/2^+$ yrast states were measured using the RDDS method applied to the detectors at 157.6° and 133.6°. Typical spectra and the time-behaviour evolution with the target-to-degrader distance at 157.6° of the 280 keV and 479 keV γ-ray transitions are illustrated in Fig. 2 (a) and (b), respectively. The lifetimes were extracted by means of the Differential Decay Curve Method (DDCM) for the singles case [24,31] which is a variation of the RDDS approach. For a level of interest, i, with a depopulating transition feeding the level, j, and populated directly from the level h, namely $h \rightarrow i \rightarrow j$, the lifetime is given by:

$$\tau_i(x) = -\frac{Q_{ij}(x) - b_{ij}\sum_h (J_{hi}/J_{ij})Q_{hi}(x)}{\frac{d}{dx}Q_{ij}(x)}\frac{1}{v}, \quad (1)$$

where $Q_{ij}(x) = I^d_{ij}(x)/(I^d_{ij}(x) + I^s_{ij}(x))$, $I^d_{ij}(x)$ and $I^s_{ij}(x)$ are the degraded and fully Doppler-shifted components of the transitions under investigation, respectively. And b_{ij} is the branching ratio of level i depopulating to j, v is the average recoil velocity and J_{hi}, J_{ij} are the relative intensities of the feeding and depopulating transitions, respectively. The derivative of $Q_{ij}(x)$ as a function of the distance, $\frac{d}{dx}Q_{ij}(x)$, was extracted using the APATHIE software [32]. The measured mean lifetimes of the $17/2^+$ and $21/2^+$ states were deduced from the statistical weighted average of the individual lifetimes at the different target-to-degrader distances within the sensitive region, as shown in Fig. 3 (a) and (b).

In a singles RDDS analysis, the lifetime of the level of interest can be influenced by unobserved feeding. As has been discussed in Refs. [31,33,34], in certain cases where the observed feeding times are not particularly long compared with the depopulating transition and the majority of the feeding is observed, it is reasonable to assume that the unobserved feeding does not significantly perturb the measured lifetime values. This assumption has been tested and validated in several measurements [35–37] where both singles and coincidence RDDS analysis were carried out, and has been applied in the present analysis. The final lifetime, τ, for each state was

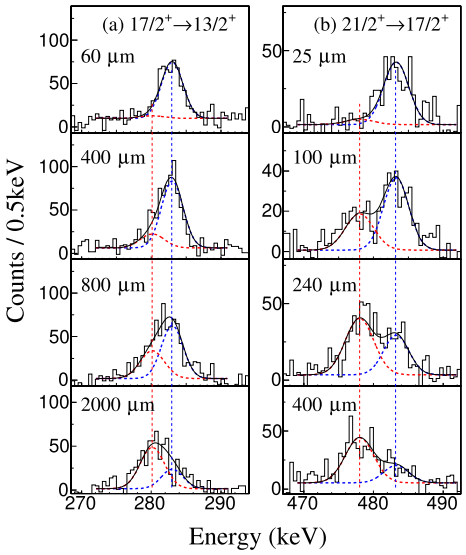

Fig. 2. Examples of RIT γ-ray singles spectra recorded at 157.6° at different target to degrader distances for (a) the 280 keV γ-ray transition depopulating the $17/2^+$ state and (b) the 478 keV transition depopulating the $21/2^+$ state in ^{169}Os. The dashed blue and red lines represent fits for the degraded and fully shifted components, respectively, while the black solid line shows the sum of the two fitted components.

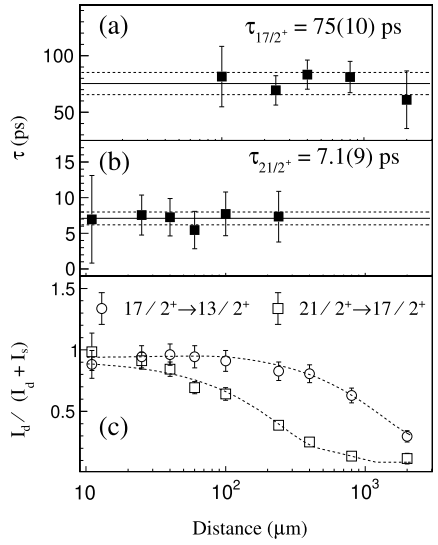

Fig. 3. Lifetimes of (a) the $17/2^+$ state and (b) the $21/2^+$ state in ^{169}Os extracted from the data recorded at 157.6° in the region of sensitivity along with the final mean lifetime (solid line) and uncertainty (dashed lines). (c) Normalized decay curves of the two excited states under study and their polynomial fit indicated by the dashed lines.

determined as the weighted average of the two values extracted separately from the data recorded at 157.6° and 133.6°. The corresponding reduced transition probability $B(E2\downarrow)$ can be deduced using the following equation:

$$B(E2\downarrow) = \frac{8.1766 \times 10^{-2}}{E_\gamma^5 \tau(1+\alpha)}\left[e^2b^2\right] \quad (2)$$

where α is the internal conversion coefficient taken from Ref. [38], E_γ is the transition energy in MeV, and τ is the extracted lifetime of the state of interest in picoseconds. The reduced transition quadrupole moments $|Q_t|$ are extracted from the $B(E2)$ values within the rotational model [39]. Assuming $K = 1/2$ for the yrast band of ^{169}Os, values of $|Q_t| = 4.3(5)$ eb and $|Q_t| = 3.7(5)$ eb

are deduced for the 280 keV and 478 keV transitions, respectively. Assuming $K = 3/2$, the corresponding transition quadrupole moments $|Q_t|$ are 4.6(5) eb and 3.9(5) eb, respectively. The final mean lifetime τ, $B(E2\downarrow)$, and $|Q_t|$ are listed in Table 1 assuming $K = 1/2$ (i.e. that the unpaired neutron mostly occupies the $1/2^+[660]$ Nilsson orbital).

3.2. ^{171}Os

The relatively large reaction cross-section for the 2p2n evaporation channel leading to the nucleus ^{171}Os made it suitable for a $\gamma\gamma$-coincidence analysis. The two separate coincident matrices for each target-to-degrader distance were obtained by sorting the recoil-gated γ-rays recorded with the Phase-I detectors at 157.6° or 133.6° on one axis and the coincident γ-rays recorded with the whole JUROGAM array on the other axis. In the present RDDS study of ^{171}Os, two types of gating procedures were used, namely gating on a depopulating transition or a feeding transition. In the latter case, unobserved side-feedings can be effectively ruled out [24].

A gate on a depopulating transition was used for the $29/2^+$ state where the gate was set on the full line shape of the 253.8 keV transition ($17/2^+ \rightarrow 13/2^+$). The method employed here to determine the lifetime is the same as the one used for the singles case (Eq. (1)), where the same assumption was made concerning the unobserved feeding. Gating on a feeding transition can eliminate the uncertainties originating from the unobserved feeding transitions effectively [24], which was used for the analysis of the other three lower yrast states. To produce the gated spectra of the $17/2^+$ and $21/2^+$ states, the gate was set on the full line shape of the 627.7 keV ($29/2^+ \rightarrow 25/2^+$) transition. For the $25/2^+$ state, the gate was set on the 644.0 keV ($33/2^+ \rightarrow 29/2^+$) transition. Typical projections of recoil-gated $\gamma\gamma$-coincidence spectra and the time-behaviour evolution with the target-to-degrader distance for the first two excited states are shown in Fig. 4. The lifetimes of the yrast $17/2^+$, $21/2^+$ and $25/2^+$ excited states were extracted using the following equation [24]:

$$\tau_i(x) = \frac{Q_{hi}(x) - Q_{ij}(x)}{\frac{d}{dx}Q_{ij}(x)}\frac{1}{v}, \qquad (3)$$

where the quantities $Q_{ij}(x)$ and $Q_{hi}(x)$ have been described in Eq. (1).

In Fig. 5 the lifetime values are shown for the yrast $17/2^+$, $21/2^+$, $25/2^+$, and $29/2^+$ states in ^{171}Os. The results were obtained within the sensitive target-to-degrader distance region using the germanium detectors placed at an angle 133.6° relative to the beam direction and the normalized decay curves $I^d_{ij}/(I^d_{ij} + I^s_{ij})$. The lifetimes measured in different conditions, the final weighted average lifetimes, as well as the corresponding transition probabilities $B(E2\downarrow)$ and quadrupole moments $|Q_t|$ are summarized in Table 1. With the $K = 3/2$ assumption for the yrast band of ^{171}Os, quadrupole moments $|Q_t| = 4.7(4)$ eb and $|Q_t| = 4.4(6)$ eb are deduced for the first two transitions, respectively. Assuming $K = 5/2$, the corresponding quadrupole moments 5.3(4) eb 4.7(6) eb for the first two transitions are obtained.

3.3. ^{173}Os

The isomeric $9/2^+$ state in ^{173}Os, shown in Fig. 1, was firstly observed and estimated to have a lifetime of several microseconds by Bark et al. [11]. An unobserved transition with an estimated energy of less than 60 keV was postulated to depopulate from the $13/2^+$ state to the $9/2^+$ state and a series of transitions were assigned as members of the favoured sequence of the $i_{13/2}$

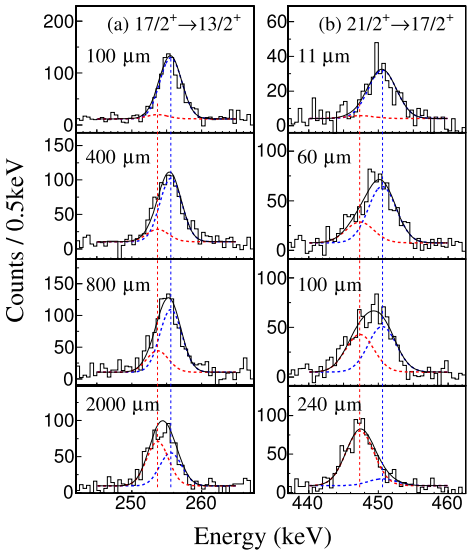

Fig. 4. Recoil-gated $\gamma - \gamma$ coincidence spectra of ^{171}Os measured at different target to degrader distances at 133.6°: (a) the $17/2^+ \rightarrow 13/2^+$ transition at 253.8 keV and (b) the $21/2^+ \rightarrow 17/2^+$ transition at 447.2 keV, after gating on the $29/2^+ \rightarrow 25/2^+$ transition at 627.7 keV.

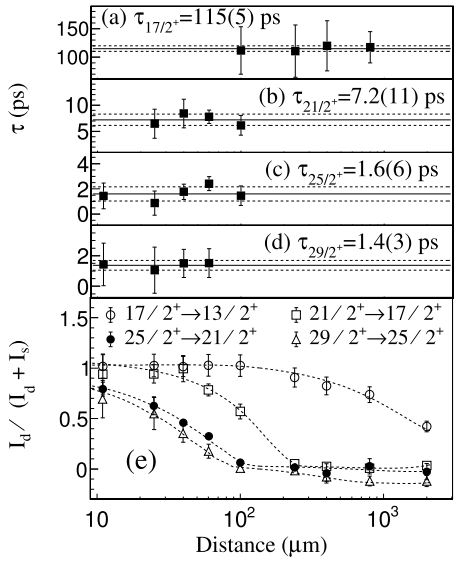

Fig. 5. Lifetimes of the (a) $17/2^+$, (b) $21/2^+$, (c) $25/2^+$ and (d) $29/2^+$ states in ^{171}Os extracted from the data recorded at 133.6° in the region of sensitivity along with the final mean lifetime (solid line) and uncertainty (dashed lines). (e) Normalized degraded intensity of the depopulating transitions for the four excited states under investigation and their polynomial fit indicated by the dashed lines.

band [11]. Subsequently, the $i_{13/2}$ band was confirmed and extended by Kalfas et al. [12]. In the present work, by employing the RIT technique, isomer-delayed 49.5 keV and 91.8 keV transitions, which were detected at the focal plane within 30 μs after the recoil implantation, were used for tagging to select the correlated prompt γ rays of ^{173}Os emitted at the target position. Due to the low production cross section via the 2p evaporation channel, the lifetimes of the first two excited states $17/2^+$ and $21/2^+$ were measured only with the detectors placed at 133.6° and then extracted by using Eq. (1).

Examples of typical spectra for the 232.7 keV and 390.2 keV transitions are illustrated in Fig. 6 and the lifetime determination of the two states is shown in Fig. 7. Assuming $K = 5/2$ for the $i_{13/2}$ band of ^{173}Os as introduced in Ref. [12], the transition quadrupole moments $|Q_t| = 5.2(5)$ eb and $|Q_t| = 6.2(12)$ eb,

Table 1
Measured lifetime values and extracted electromagnetic properties for excited states under investigation in ^{169}Os, ^{171}Os and ^{173}Os. $K = 1/2$, $K = 3/2$, and $K = 5/2$ are assumed for the $i_{13/2}$ bands of ^{169}Os, ^{171}Os, and ^{173}Os, respectively.

	E_γ (keV)	$I_i^\pi \to I_f^\pi$	Detector angle	Coincidences	Singles	Average values		
				τ_i (ps)		τ (ps)	$B(E2\downarrow)$ (W.u.)	$\lvert Q_t\rvert$ (eb)
^{169}Os	280	$17/2^+ \to 13/2^+$	133.6°		72(5)			
			157.6°		75(10)			
						74(9)	104(15)	4.3(5)
	478	$21/2^+ \to 17/2^+$	133.6°		6.9(12)			
			157.6°		7.1(9)			
						7.0(10)	82(12)	3.7(5)
^{171}Os	253.8	$17/2^+ \to 13/2^+$	133.6°	115(5)				
			157.6°	106(10)				
						110(9)	109(9)	4.7(4)
	447.2	$21/2^+ \to 17/2^+$	133.6°	7.2(11)				
			157.6°	7.7(10)				
						7.5(10)	105(14)	4.4(6)
	566.8	$25/2^+ \to 21/2^+$	133.6°	1.6(6)				
			157.6°	1.9(6)				
						1.7(5)	140(50)	4.6(16)
	627.7	$29/2^+ \to 25/2^+$	133.6°		1.4(3)			
			157.6°		1.3(4)			
						1.3(4)	110(25)	4.3(11)
^{173}Os	232.7	$17/2^+ \to 13/2^+$	133.6°		172(15)	172(15)	101(9)	5.2(5)
	390.2	$21/2^+ \to 17/2^+$	133.6°		8.5(16)	8.5(16)	180(35)	6.2(12)

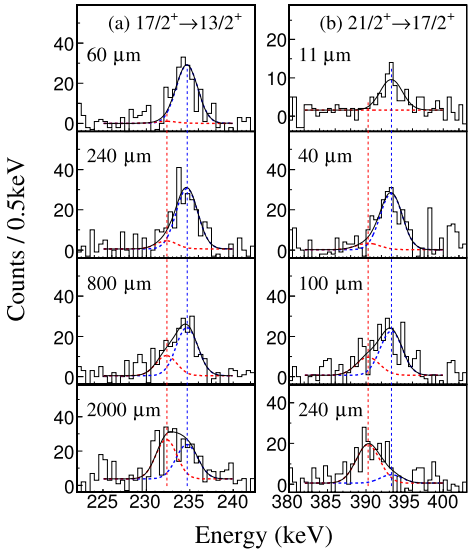

Fig. 6. Examples of RIT γ-ray singles spectra measured at 133.6° to the beam axis for (a) the 232.7 keV transition depopulating the $17/2^+$ state and (b) the 390.2 keV transition depopulating the $21/2^+$ state in ^{173}Os.

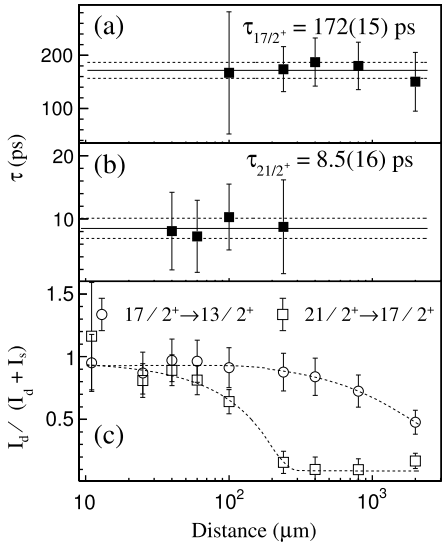

Fig. 7. Lifetimes of the (a) $17/2^+$ and (b) $21/2^+$ states in ^{173}Os at 133.6° in the region of sensitivity along with the final mean lifetime (solid line) and uncertainty (dashed lines). (c) Normalized decay curves of the two excited states under investigation and their polynomials fit indicated by the dashed lines.

for the $17/2^+ \to 13/2^+$ and $21/2^+ \to 17/2^+$ transitions, respectively, are obtained within the rotational model [39] and given in Table 1 together with the mean lifetimes and the corresponding transition probabilities $B(E2\downarrow)$. With the $K = 3/2$ assumption, the corresponding quadrupole moments for these two transitions $|Q_t| = 4.6(4)$ eb and $|Q_t| = 5.8(11)$ eb are deduced.

4. Discussion

Excitation energy ratios, $E_{4_1^+}/E_{2_1^+}$ for even-mass Os isotopes and $(E_{21/2^+} - E_{13/2^+})/(E_{17/2^+} - E_{13/2^+})$ for the $\nu i_{13/2^+}$ bands in odd-mass Os isotopes, are shown in Fig. 8(a). The energy ratios are compared with predictions for a harmonic vibrator and the collective model for rigid axial and gamma-soft triaxial rotors [2,44]. While the energy ratios for the even and odd-N isotopes follow each other rather closely as a function of neutron number until $N = 98$, a bifurcation between the even and odd-mass isotopes appears for $N > 98$. After this point, the $E_{4_1^+}/E_{2_1^+}$ ratios for the even-mass isotopes start deviating from the $(E_{21/2^+} - E_{13/2^+})/(E_{17/2^+} - E_{13/2^+})$ ratios for the $\nu i_{13/2^+}$ bands, demonstrating the entry into a regime where the odd valence quasineutron is strongly coupled to the even-even core. For neutron numbers $N < 98$, the odd $i_{13/2^+}$ valence neutron is decoupled from the core and does not essentially affect the relative excitation energies within the $\nu i_{13/2^+}$ bands. With the exception of ^{163}W [45], a similar trend is found in the neighbouring W isotopic chain (see below). In Fig. 8(b) the experimental $B(E2; 17/2^+ \to 13/2^+)$ values for $\nu i_{13/2^+}$ bands in the odd-mass Os isotopes are compared with the $B(E2; 2_1^+ \to 0_{gs}^+)$ values for the even-mass Os isotopes. In Fig. 8(c) ratios of the $B(E2\downarrow)$ values: $B(E2; 21/2^+ \to 17/2^+)/B(E2; 17/2^+ \to 13/2^+)$ for the $\nu i_{13/2^+}$ bands in the odd-N Os isotopes and $B(E2; 4_1^+ \to 2_1^+)/B(E2; 2_1^+ \to 0_{gs}^+)$ for even-N isotopes are shown. The ratios of reduced transition probabilities, $B_{4/2}$, in the lightest even-mass osmium isotopes and other neutron-deficient tungsten and platinum nuclei are known to reveal apparently "anomalous" val-

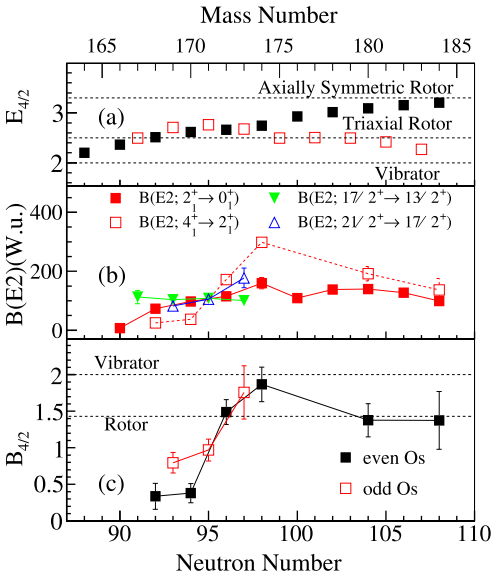

Fig. 8. (a) Ratios between the excitation energies of the first excited 4^+ and 2^+ states for even-mass Os isotopes (black filled squares) compared with the corresponding ratios for the $21/2^+$ and $17/2^+$ states relative to the $13/2^+$ state for odd-mass Os isotopes (red open squares). (b) Experimental $B(E2\downarrow)$ values for the even Os isotopes (squares) and for the odd Os isotopes (triangles) (c) Ratios of $B(E2\downarrow)$ values: $B(E2; 21/2^+ \rightarrow 17/2^+)/B(E2; 17/2^+ \rightarrow 13/2^+)$ for odd-N isotopes and $B(E2; 4_1^+ \rightarrow 2_1^+)/B(E2; 2_1^+ \rightarrow 0_{gs}^+)$ for even-N isotopes. Predictions for a harmonic vibrator and collective models for axial and γ-soft triaxial rotors [2,44] are shown as dashed lines. The experimental $B(E2\downarrow)$ values for ^{169,171,173}Os have been measured in the present work, ^{168}Os is taken from Ref. [13], ^{170}Os from Ref. [14] and the rest from Refs. [40–43].

ues that cannot be reproduced in terms of the collective rotational model [5,13–15]. Of the presently obtained new $B_{4/2}$ ratios in ^{169,171,173}Os, the $B_{4/2}$ values for ^{169}Os and ^{171}Os deviate clearly from the expectations for collective excitations. The ratio $B_{4/2}(^{169}\text{Os}) = 0.79(16)$ might also be considered "anomalous", even though it, interestingly, seems to be significantly larger than for its even-N nearest neighbours ^{168}Os and ^{170}Os. Turning to the Interacting Boson Model, "microscopic" predictions of collective behaviour in the W, Os, and Pt nuclei of interest can be studied. Fig. 9 shows $B(E2\downarrow)$ values and $B_{4/2}$ ratios as a function of the boson quantum number $N_b = (N_N + N_P)/2$, where N_N and N_P are the number of neutrons and proton holes relative to the closed-shell neutron or proton number 82 (for neutron numbers > 104 the closed shell at 126 is chosen as a reference). The $B(E2)$ values, as shown in Fig. 9 (a), follow the expected increasing trend as a function of increasing valence pair number with a saturation around the middle of the neutron $N = 82 - 110$ shell ($N_b > 10$), and also reveal the expected tendency of increasing collectivity with the neutron-proton valence number product $N_N \times N_P$ [54] which in this case for a given N_b is successively larger for smaller Z, i.e. larger for tungsten than osmium and larger for osmium than platinum.

The $B_{4/2}$ ratios in Fig. 9 (b) are compared with the predictions for the U(5) (vibrational), O(6) (γ-soft triaxial rotor), and SU(3) (axial rotor) limits of the IBM. The $B_{4/2}$ ratios exhibit the previously noted and unexpected "phase transition" for $N_b \approx 8 - 10$ between an apparently non-collective and a collective regime [5,13–15]. The results obtained in the present work show that both the $B(E2; 17/2^+ \rightarrow 13/2^+)$ values and the $B(E2; 21/2^+ \rightarrow 17/2^+)/B(E2; 17/2^+ \rightarrow 13/2^+)$ ratios for ^{169,171,173}Os follow, within experimental uncertainties, those of the corresponding $B(E2)$ values and $B_{4/2}$ ratios in the neighbouring even-N isotopes, as expected from the similar energy ratios and consistent with the decoupling of the odd $i_{13/2^+}$ valence neutron from the core. This accordingly indicates that the odd $i_{13/2^+}$ valence neutron has little effect on the electric quadrupole strength. In the recent work of Lewis et al. [45], lifetime measurements for the $21/2^+$ and $17/2^+$ states in the $\nu i_{13/2^+}$ band of ^{163}W were reported. As can be seen in Fig. 9 (b), the $B_{4/2}$ ratio reported for ^{163}W [45], although with a relatively large experimental uncertainty, stands out and deserves further attention. Furthermore, the reported $B_{4/2}$ ratio for ^{163}W is in better agreement with the collective vibrational limit rather than a collectively rotating system as was proposed in Ref. [45]. Lewis et al. [45] also argued that the core polarising effect of the $i_{13/2^+}$ valence neutron would influence the $B_{4/2}$ ratio in ^{163}W by making it adopt an axial prolate shape. This, however, is not likely since its $B(E2; 17/2^+ \rightarrow 13/2^+)$ value lies right in between the $B(E2; 2_1^+ \rightarrow 0_g^+)$ values for the closest even-N W isotopes ^{162}W and ^{164}W [16] and follows the observed systematic dependence on N_b rather well. Furthermore, the energy ratio $(E_{21/2^+} - E_{13/2^+})/(E_{17/2^+} - E_{13/2^+})$ for ^{163}W also lies in between the corresponding $E_{4_1^+}/E_{2_1^+}$ ratios for the nearest even-mass W isotopes [55–57]. We also note that the $B(E2; 17/2^+ \rightarrow 13/2^+)$ and $B(E2; 21/2^+ \rightarrow 17/2^+)$ values measured for ^{167}W [46] are found to agree well with the systematic trends in the tungsten isotopes. In Ref. [45] the anomalous $B_{4/2}$ ratios previously observed in neutron deficient W and Pt nuclei [5,15] were attributed to their γ-soft triaxial shapes for which the projected angular momentum quantum, K, is not a conserved quantum number. Such effects are, however, included in the predictions from collective models for triaxial and γ-soft rotors (see, e.g., Refs. [2,44]).

In principle, shape coexistence cannot be excluded as a possible cause for an "anomalous" $B_{4/2} < 1$ if, for example, a smooth transition to a less collective structure would occur as a function of increasing angular momentum in the yrast band. However, such a phenomenon might be considered rather remarkable in itself and we are not aware of any reports of cases in the literature where $B_{4/2} < 1$ within the relatively wide and well-known region of Os-Pt-Hg nuclei exhibiting shape coexistence near the ground state. For instance, two cases close to the nuclei of interest in this work where shape coexistence has been extensively discussed are ^{172}Os [58] and ^{176}Pt [59,60] for which the measured $B_{4/2}$ ratios are $B_{4/2} = 1.49(17)$ [17] and $B_{4/2} = 1.86(25)$ [59], respectively. In the osmium isotopes, manifestations of coexistence of different quadrupole-deformed shapes have been associated with an early upbend in the yrast band. This happens at spin $I \approx 6\hbar$ in the yrast ground-state band of ^{172}Os [58], which was successfully interpreted based on a phenomenological band mixing model [11,61–63]. In the more neutron deficient Os isotopes ^{171}Os [10], ^{170}Os [61], and ^{168}Os [64], band mixing calculations suggested that as the neutron number decreases toward the $N = 82$ closed shell, the deformed prolate intruder band is shifted to increasingly higher excitation energies relative to the weakly deformed ground-state band. Based on this systematic trend it is not anticipated that shape coexistence will play an important role in the low-lying yrast structures in Os isotopes with $N < 96$ and even less likely that it will lead to the ratio $B_{4/2} < 1$.

We conclude that the enigma of anomalous $B_{4/2}$ ratios in the region of heavy, neutron deficient transitional nuclei appears to remain unexplained by theory. Furthermore, the present work indicates that the addition of an odd $i_{13/2^+}$ valence neutron has little effect on either the $B(E2)$ value or the $B_{4/2}$ ratio of these even-N systems.

5. Summary

The lifetimes of the first excited $17/2^+$ and $21/2^+$ states in the neutron-deficient osmium isotopes ^{169,171,173}Os as well as the $25/2^+$ and $29/2^+$ states in ^{171}Os have been measured using the

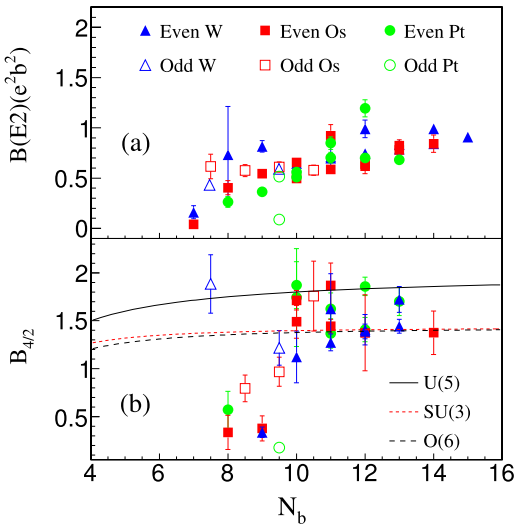

Fig. 9. Experimental $B(E2\downarrow)$ values (a), Ratios of $B(E2\downarrow)$ values and comparison with different IBM limits (b), for W, Os, and Pt isotopes as a function of the valence pair parameter $N_b = (N_N + N_P)/2$ (see text and legend for further details). The experimental data are from the present work and Refs. [5,13–17,40–43,45–53].

recoil distance Doppler shift technique. The corresponding $B(E2)$ values for the $21/2^+ \rightarrow 17/2^+$ and $17/2^+ \rightarrow 13/2^+$ electromagnetic transitions follow the same unusual trend as observed in the neighbouring even-N osmium isotopes. The deduced low value for the ratio $B_{4/2} = 0.79(16)$ in ^{169}Os might also be considered to join the group of "anomalous" $B(E2)$ ratios observed for members of the even-N tungsten, osmium and platinum isotopes [5,13–15] with similar neutron numbers. It is concluded that the decoupled $i_{13/2^+}$ valence neutron appears to act mainly as a "spectator", also with respect to the appearance of anomalous $B_{4/2}$ ratios in the most neutron deficient osmium isotopes.

Declaration of competing interest

The authors declare that they have no known competing financial interests or personal relationships that could have appeared to influence the work reported in this paper.

Acknowledgements

This work was supported by the Swedish Research Council under Grant No. 2019-04880, the United Kingdom Science and Technology Facilities Council (STFC), the EU 7th Framework Programme, Integrating Activities Transnational Access, project No. 262010 ENSAR, and the Academy of Finland under the Finnish Centre of Excellence Programme (Nuclear and Accelerator Based Physics Programme at JYFL). E.I., Y.D.F., and M.K.R. acknowledge support from the International Joint Research Promotion Program of Osaka University. W. Zhang acknowledges support from the China Scholarship Council under grant No. 201700260239. The authors acknowledge the support of the GAMMAPOOL for the JUROGAM detectors.

References

[1] J.L. Wood, Nuclear collectivity – its emergent nature viewed from phenomenology and spectroscopy, in: Emergent Phenomena in Atomic Nuclei from Large-Scale Modeling, World Scientific, Singapore, 2017.
[2] A. Bohr, B.R. Mottelson, Nuclear Structure, vol. II, 45, World Scientific, Singapore, 1998.
[3] R.F. Casten, Nuclear Structure from a Simple Perspective, Oxford University Press, New York, 2000.
[4] F. Iachello, A. Arima, The Interacting Boson Model, Cambridge University Press, ISBN 978-0-511-89551-7, 1987.
[5] B. Cederwall, et al., Phys. Rev. Lett. 121 (2018) 022502.
[6] J. Wood, K. Heyde, W. Nazarewicz, M. Huyse, P. van Duppen, Phys. Rep. 215 (3) (1992) 101–201.
[7] K. Heyde, J.L. Wood, Rev. Mod. Phys. 83 (2011) 1467, Erratum: Rev. Mod. Phys. 83 (2011) 1655.
[8] D.T. Joss, et al., Phys. Rev. C 66 (2002) 054311.
[9] A.M. Thornthwaite, Ph.D. thesis, University of Liverpool, 2014 (unpublished).
[10] R.A. Bark, et al., Nucl. Phys. A 646 (1999) 399.
[11] R.A. Bark, G.D. Dracoulis, A.E. Stuchbery, Nucl. Phys. A 514 (1990) 503.
[12] C.A. Kalfas, et al., Nucl. Phys. A 526 (1991) 205.
[13] T. Grahn, et al., Phys. Rev. C 94 (2016) 044327.
[14] A. Goasduff, et al., Phys. Rev. C 100 (2019) 034302.
[15] B. Saygi, et al., Phys. Rev. C 96 (2017) 021301(R).
[16] M. Doncel, et al., Phys. Rev. C 95 (2017) 044321.
[17] A. Virtanen, N.R. Johnson, F.K. McGowan, I.Y. Lee, C. Baktash, M.A. Riley, J.C. Wells, J. Dudek, Nucl. Phys. A 591 (1995) 145.
[18] M.J. Taylor, et al., Nucl. Instrum. Methods Phys. Res., Sect. A 707 (2013) 143.
[19] M. Leino, et al., Nucl. Instrum. Methods Phys. Res., Sect. B 99 (1995) 653.
[20] R.D. Page, et al., Nucl. Instrum. Methods Phys. Res., Sect. B 204 (2003) 634.
[21] C.W. Beausang, et al., Nucl. Instrum. Methods Phys. Res., Sect. A 313 (1992) 37.
[22] G. Duchêne, et al., Nucl. Instrum. Methods Phys. Res., Sect. A 432 (1999) 90.
[23] A.N. Andreyev, et al., Nucl. Instrum. Methods Phys. Res., Sect. A 533 (2004) 422.
[24] A. Dewald, O. Möller, P. Petkov, Prog. Part. Nucl. Phys. 67 (2012) 786.
[25] I.H. Lazarus, et al., IEEE Trans. Nucl. Sci. 48 (2001) 567.
[26] P. Rahkila, et al., Nucl. Instrum. Methods Phys. Res., Sect. A 595 (2008) 637.
[27] D.C. Radford, Nucl. Instrum. Methods Phys. Res., Sec. A 361 (1995) 306.
[28] C. Scholey, D.M. Cullen, E.S. Paul, et al., Recoil-Isomer Tagging Techniques at RITU, Exotic Nuclei and Atomic Masses, Springer, 2003, p. 494.
[29] E.S. Paul, et al., Phys. Rev. C 51 (1995) 78.
[30] R.D. Page, et al., Phys. Rev. C 53 (1996) 660.
[31] A. Dewald, S. Harissopulos, P. Brentano, Z. Phys. A 334 (1989) 163.
[32] F. Seiffert, Program APATHIE, Institut für Kernphysik, Universitat zu Köln, 1989 (unpublished).
[33] T. Grahn, et al., Phys. Rev. Lett. 97 (2006) 062501.
[34] T. Grahn, et al., Nucl. Phys. A 801 (2008) 83.
[35] S. Harissopulos, et al., Nucl. Phys. A 467 (1987) 528.
[36] P. Petkov, et al., Nucl. Phys. A 543 (1992) 589.
[37] P. Petkov, et al., Phys. Rev. C 62 (2000) 014314.
[38] T. Kibédi, et al., Nucl. Instrum. Methods Phys. Res., Sect. A 589 (2008) 202.
[39] A. Bohr, B.R. Mottelson, Nuclear Structure, vol. II, 45, World Scientific, Singapore, 1998.
[40] D. O'Donnell, et al., Phys. Rev. C 79 (2009) 064309.
[41] S. Stolze, Ph.D. thesis, University of Jyväskylä, 2017 (unpublished).
[42] O. Möller, et al., Phys. Rev. C 72 (2005) 034306.
[43] https://www.nndc.bnl.gov/.
[44] A.S. Davydov, G.F. Filippov, Nucl. Phys. 8 (1958) 237.
[45] M.C. Lewis, et al., Phys. Lett. B 798 (2019) 134998.
[46] C.B. Li, et al., Phys. Rev. C 94 (2016) 044307.
[47] V. Werner, et al., Phys. Rev. C 93 (2016) 034323.
[48] J.-M. Regis, et al., Nucl. Inst. Methods A 606 (2009) 466.
[49] M. Rudigier, J.-M. Regis, J. Jolie, K.O. Zell, C. Fransen, Nucl. Phys. A 847 (2010) 89.
[50] J.C. Walpe, et al., Phys. Rev. C 85 (2012) 057302.
[51] C.B. Li, et al., Phys. Rev. C 90 (2014) 047302.
[52] C. Müller-Gatermann, et al., Phys. Rev. C 97 (2018) 024336.
[53] H. Watkins, Ph.D. thesis, University of Liverpool, 2011 (unpublished).
[54] R.F. Casten, Nucl. Phys. A 443 (1985) 1.
[55] H.J. Li, et al., Phys. Rev. C 92 (2015) 014326.
[56] D.T. Joss, et al., Phys. Rev. C 93 (2016) 024307.
[57] J. Simpson, et al., J. Phys. G 18 (1992) 1207.
[58] J.L. Durell, G.D. Dracoulis, C. Fahlander, A.P. Byrne, Phys. Lett. B 115 (1982) 367.
[59] G.D. Dracouhs, et al., J. Phys. G 12 (1986) L97.
[60] B. Cederwall, et al., Z. Phys. A 337 (1990) 283.
[61] G.D. Dracoulis, R.A. Bark, A.E. Stuchbery, A.P. Byrne, A.M. Baxter, F. Riess, Nucl. Phys. A 486 (1988) 414.
[62] P.M. Davidson, et al., Nucl. Phys. A 568 (1994) 90.
[63] G.J. Lane, et al., Nucl. Phys. A 589 (1995) 129.
[64] D.T. Joss, et al., Nucl. Phys. A 689 (2001) 631.